TJVS Turkish Journal of Vascular Surgery

Turk J Vasc Surg.2026;35(1):7-13
DOI: 10.9739/tjvs.2025.09.054

Available online at www.turkishjournalofvascularsurgery.org

Original Article

Dapagliflozin attenuates histopathological alterations in a rat model of abdominal aortic aneurysm

Mustafa Baris Kemahli[1], Cuneyt Narin[1], Cagatay Bilen[2], Pinar Akokay[3], Tugra Gencpinar[4], Kivanc Metin[4], Serdar Bayrak[4]

[1]Acıbadem İzmir Kent Hospital, Department of Cardiovascular Surgery, İzmir, Türkiye
[2]Aydın Adnan Menderes University, Faculty of Medicine, Department of Cardiovascular Surgery, Aydın, Türkiye
[3]Kavram Vocational School, Department of Histology, İzmir, Türkiye
[4]Dokuz Eylül University, Faculty of Medicine, Department of Cardiovascular Surgery, İzmir, Türkiye

Received: September 24, 2025 Accepted: November 12, 2025 Published online: January 12, 2026

Abstract

Aim: Abdominal aortic aneurysm is a progressive enlargement of the abdominal aorta associated with high mortality risk. Despite advances in surgical and endovascular treatments, no pharmacological therapy has been established to prevent aneurysm growth. Dapagliflozin, a sodium–glucose cotransporter-2 inhibitor, has demonstrated cardiovascular benefits beyond glycemic control. The aim of this study was to investigate the effects of dapagliflozin in a calcium phosphate–induced rat model of abdominal aortic aneurysm.

Material and Methods: Twenty male Wistar albino rats were randomly divided into three groups: sham operated rats (Sham, n=6), rats with abdominal aortic aneurysm induced by calcium phosphate (AAA, n=7), and rats with aneurysm treated with dapagliflozin (Dapagliflozin group, n=7). Aneurysm formation was induced by periaortic application of calcium phosphate. The Dapagliflozin group received daily oral dapagliflozin at a dose of 1 mg/kg for 28 days. Morphometric parameters including lumen area, lumen plus intima area, and lumen plus intima plus media area were evaluated using hematoxylin–eosin staining. Elastin degradation was assessed with Van Gieson staining, vascular calcification with Alizarin Red staining, and apoptosis with immunohistochemical detection of Caspase-3 and Caspase-9. Statistical analyses were performed using Student's t-test and Mann–Whitney U test, with a significance threshold of $p<0.05$.

Results: Morphometric parameters were significantly increased in the AAA group compared with the Sham group (all $p<0.001$). These parameters were reduced in the Dapagliflozin group compared with the AAA group (all $p<0.001$). Elastin degradation and calcium deposition were higher in the AAA group compared with Sham ($p=0.001$ and $p=0.002$) and decreased with dapagliflozin treatment ($p=0.001$ and $p=0.012$). Caspase-3 and Caspase-9 expression was elevated in the AAA group ($p=0.002$ and $p=0.003$) and decreased in the Dapagliflozin group, although the reduction in Caspase-9 did not reach statistical significance ($p=0.068$).

Conclusion: Dapagliflozin reduced aortic dilatation, elastin degradation, vascular calcification, and Caspase-3–mediated apoptosis in a calcium phosphate–induced rat model of abdominal aortic aneurysm. These findings suggest that dapagliflozin exerts protective effects on vascular integrity beyond glucose regulation and may represent a potential medical therapy for abdominal aortic aneurysm.

Keywords: Abdominal aortic aneurysm, dapagliflozin, sodium-glucose transporter 2 inhibitors, elastin, aneurysm

INTRODUCTION

Abdominal aortic aneurysm (AAA) is defined as a permanent dilation of the abdominal aorta measuring at least 1.5 times the normal diameter [1]. Its prevalence varies across regions, with recent estimates reporting a global rate of 0.92% among individuals aged 30–79 years, affecting men three to four times more frequently than women and increasing with age.

CITATION
Kemahli MB, Narin C, Bilen C, Akokay P, Gencpinar T, Metin K, et al. Dapagliflozin attenuates histopathological alterations in a rat model of abdominal aortic aneurysm. Turk J Vasc Surg.2026;35(1):7-13.

Corresponding Author: Mustafa Baris Kemahli, Acıbadem İzmir Kent Hospital, Department of Cardiovascular Surgery, İzmir, Türkiye
Email: bariskemahli@hotmail.com

Established risk factors include advanced age, male sex, smoking, hypertension, hypercholesterolemia, and a positive family history [2]. Despite advances in imaging, screening, and surgical or endovascular interventions, no approved pharmacological therapy exists to halt aneurysm progression or rupture [3].

The pathogenesis of AAA involves a complex interplay of extracellular matrix degradation, vascular smooth muscle cell loss and apoptosis, chronic inflammation, and oxidative stress. Histologically, aneurysmal walls are characterized by elastin fragmentation, medial smooth muscle cell depletion, fibrosis, and progressive vascular calcification [3].

Animal models have been instrumental in clarifying the cellular and molecular mechanisms underlying AAA formation. The calcium chloride ($CaCl_2$) model reliably induces medial degeneration and inflammation, while the calcium phosphate ($CaPO_4$) model accelerates aneurysm formation, leading to marked elastin degradation, apoptosis, and calcification within a short period [4–6]. This reproducible and inflammation-driven model provides a robust platform for experimental pharmacological studies.

Sodium–glucose cotransporter-2 (SGLT2) inhibitors, such as dapagliflozin, are oral antidiabetic agents that have shown significant cardiovascular benefits beyond glycemic control. Large randomized trials demonstrated reduced risk of cardiovascular death or worsening heart failure, even in patients without diabetes [7]. The underlying mechanisms are thought to include attenuation of oxidative stress, suppression of inflammation, prevention of fibrosis, and modulation of cellular apoptosis [8]. However, the potential effects of dapagliflozin in the $CaPO_4$-induced AAA model remain unknown.

Despite the increasing understanding of the molecular mechanisms underlying aneurysm formation, there is still no pharmacological therapy that effectively prevents disease progression. Recent studies have suggested that metabolic modulators, including sodium–glucose cotransporter-2 (SGLT2) inhibitors, may exert vasculoprotective and anti-inflammatory effects independent of their glucose-lowering actions. Based on these observations, we hypothesized that dapagliflozin could attenuate structural wall degeneration, elastin loss, and calcification in the calcium phosphate–induced model of abdominal aortic aneurysm. Therefore, the present study aimed to investigate the effects of dapagliflozin on lumen morphology, vascular diameter, elastin preservation, and vascular calcification in a rat model of $CaPO_4$-induced abdominal aortic aneurysm.

MATERIAL AND METHODS

This experimental study was conducted on 20 male Wistar albino rats weighing 300 g. The animals were obtained from the Dokuz Eylul University Laboratory Animal Research Center. They were housed under standard laboratory conditions (22±2 °C, 55±10% humidity, 12-hour light/dark cycle) with free access to standard chow and water ad libitum. The study protocol was approved by the Dokuz Eylul University Local Ethics Committee for Animal Experiments and was performed in accordance with the Guide for the Care and Use of Laboratory Animals. The study was designed and reported in accordance with the ARRIVE (Animal Research: Reporting of In Vivo Experiments) guidelines to ensure methodological transparency and reproducibility. Rats were randomly divided into three groups. Animals were randomly assigned to experimental groups using a computer-generated simple randomization sequence. AAA and DAPA groups each included seven rats, while the Sham group included six rats.

Sham group (Sham): Laparotomy and periaortic application of 0.9% NaCl without aneurysm induction. AAA group (AAA): Aneurysm induction with calcium phosphate.

AAA+Dapagliflozin treatment group (DAPA): Aneurysm induction with calcium phosphate followed by daily dapagliflozin treatment.

Experimental Protocol

Anesthesia and analgesia were achieved with ketamine (50 mg/kg) and xylazine (10 mg/kg). Antibiotic prophylaxis was administered with cefazolin (50 mg/kg). Following appropriate skin preparation, a laparotomy was performed. The abdominal aorta was isolated from surrounding tissues. In the AAA and DAPA groups, a sterile sponge soaked in 0.5 mol/L calcium chloride solution was wrapped around the isolated aorta for 10 minutes, followed by the application of a sponge soaked in phosphate-buffered saline (PBS) to the same area for 5 minutes. In the Sham group, instead of calcium chloride and PBS, a sponge soaked in 0.9% NaCl was applied to the aorta for 15 minutes. All laparotomies were subsequently closed. In the treatment group (DAPA), starting from the day of surgery, dapagliflozin was administered by oral gavage once daily at a dose of 1 mg/kg for 28 days. At the end of the 28-day follow-up, the animals were re-anesthetized with ketamine (50 mg/kg) and xylazine (10 mg/kg). A laparotomy was performed, and the infrarenal aortic segment was harvested. The animals were euthanized by exsanguination. Aortic specimens were fixed in 10% buffered formalin for histological and immunohistochemical analyses.

Evaluated Parameters

The primary endpoint of the study was the reduction in aortic dilatation parameters, including lumen area, lumen + intima area, and lumen+intima+media area. These morphometric indices were considered the principal measurements reflecting aneurysmal progression. Secondary endpoints comprised histopathological indicators such as elastin degradation, vascular calcification, and apoptosis-related Caspase-3 and Caspase-9 expression. Morphometric indices: lumen area, lumen+intima area, lumen+intima+media area. Structural alterations: elastin

degeneration, calcium deposition. Apoptotic activity: Caspase-3 and Caspase-9 expression. Routine Light Microscopic Protocol Tissues were fixed in 10% buffered formalin for 48–72 h, dehydrated through graded alcohols, cleared with xylene, and embedded in paraffin. Sections of 5 μm thickness were obtained using a rotary microtome (Leica RM 2255, Nussloch, Germany) and mounted on poly-L-lysine–coated slides. The sections were deparaffinized, rehydrated, and stained with hematoxylin and eosin, Masson's trichrome, Alizarin Red, and Van Gieson. Images were analyzed using a computer-assisted image analysis system consisting of a microscope (BX-51, Olympus, Tokyo, Japan) equipped with a high-resolution video camera (DP-71, Olympus, Tokyo, Japan). Parameters such as lumen area and lumen diameter were evaluated using hematoxylin and eosin staining, and measurements were performed with ImageJ software. Elastin degradation was evaluated using Van Gieson staining and scored as follows:

1= mild elastin degradation

2= moderate degradation

3= moderate to severe degradation

4= severe degradation

Vascular calcification was assessed using Alizarin Red staining. Calcium deposition in the medial layer was evaluated semi-quantitatively under light microscopy. The extent of calcification was scored independently by two blinded observers according to the following grading system:

0= no visible calcification,

1= mild, focal calcification,

2= moderate calcification involving larger areas,

3= extensive and diffuse calcification across the vessel wall.

Detection and Evaluation of Apoptosis Immunohistochemistry was performed using the streptavidin–biotin method. Sections were placed on lysine-coated slides, incubated overnight at 60°C, deparaffinized in xylene, and rehydrated through graded alcohols. Antigen retrieval was carried out with 10 mM citrate buffer at 95°C for 5 min. Sections were circumscribed with a Dako pen (Dako Aps, Glostrup, Denmark) and incubated with 3% hydrogen peroxide at 37°C for 15 min to block endogenous peroxidase activity. After incubation with normal serum blocking solution for 30 min, sections were exposed to primary antibodies against Caspase-3 (BiossUSA, Woburn, MA, USA; monoclonal antibody, cat. no. bsm-33284M) and Caspase-9 (BiossUSA, polyclonal antibody, cat. no. BS-0049R) overnight in a humid chamber (30–60%). The following day, sections were washed with phosphate-buffered saline (PBS), incubated with biotinylated immunoglobulin G, and then treated with streptavidin–peroxidase conjugate (SensiTek, West Logan, USA; HRP Anti-Polyvalent Lab Pack, cat. no. SHP125). After three washes in PBS, immunoreactivity was visualized using 3,3'-diaminobenzidine (Roche Diagnostics, Basel, Switzerland; cat. no. 11718096001) for 2 min. Sections were counterstained with Mayer's hematoxylin (Sigma Aldrich, Ohio, USA) for 10 sec and mounted with Entellan (Merck, Darmstadt, Germany).

Scoring of Active Caspase-3 and Caspase-9 Semi-quantitative analysis of immunostaining was performed using the following grading system:

0= no immunoreactivity

1= very little positive staining, mild intensity

2= moderate positive staining (between grade 1 and grade 3)

3= strong, evenly distributed positive staining across the entire image.

All histological and immunohistochemical evaluations were performed by two independent observers blinded to the experimental groups, and the average score was used to represent the degree of immunostaining for each aortic section.

Statistical Analysis

Continuous variables, including lumen area, lumen+intima+media area, and lumen+intima area, were expressed as mean ± standard deviation (SD). The distribution of data was assessed using the Shapiro–Wilk test to evaluate normality. Equality of variances was verified with Levene's test before performing parametric analyses. Between-group comparisons were conducted using the independent samples Student's t-test for normally distributed variables, and Welch's correction was applied when the assumption of equal variances was not satisfied. Ordinal variables, namely Caspase-3, Caspase-9, Van Gieson elastin degradation scores, and calcium deposition grades, were summarized as median values with interquartile ranges (IQR). Group comparisons for these variables were carried out using the Mann–Whitney U test for non-normally distributed or ordinal data. Statistical significance was defined as $p<0.05$, with very small values reported as $p<0.001$. All analyses were performed using IBM SPSS Statistics for Windows, Version 25.0 (IBM Corp., Armonk, NY, USA) under an institutional academic license. Exact p values were provided for all comparisons where available; for tests yielding probabilities below 0.001, the values were reported as $p<0.001$ according to the statistical output.

RESULTS

Lumen area, lumen+intima area, and lumen+intima+media area were all significantly larger in the AAA group compared with sham (all $p<0.001$). Dapagliflozin treatment markedly reduced these parameters compared with AAA (all $p<0.001$). The sham–DAPA comparison did not reach statistical significance for lumen area ($p=0.129$) and lumen+intima area ($p=0.070$), whereas lumen+intima+media area remained significantly higher in DAPA compared with sham ($p=0.002$) (Table 1) (Figure 1).

Table 1. Morphometric parameters (Mean ± SD, Student's t-test)

Parameter	Sham	AAA	DAPA	p (Sham–AAA)	p (Sham–DAPA)	p (AAA–DAPA)
Lumen area	200879.65±46088.55	476383.50±38501.24	274589.01±100819.71	**<0.001**	0.129	**<0.001**
Lumen+intima area	226895.11±37018.45	560368.40±47164.42	305766.08±89678.77	**<0.001**	0.070	**<0.001**
Lumen+intima+media area	434068.55±81284.07	822403.49±44826.69	624316.25±83187.51	**<0.001**	0.002	**<0.001**

Data are presented as mean ± standard deviation (SD). Exact p values are provided for all comparisons where available; for tests yielding very small probabilities (below 0.001), the values are reported as p<0.001 according to the statistical output. Values of p<0.05 were considered statistically significant. Sham: sham-operated control group, AAA: abdominal aortic aneurysm group, DAPA: dapagliflozin-treated group

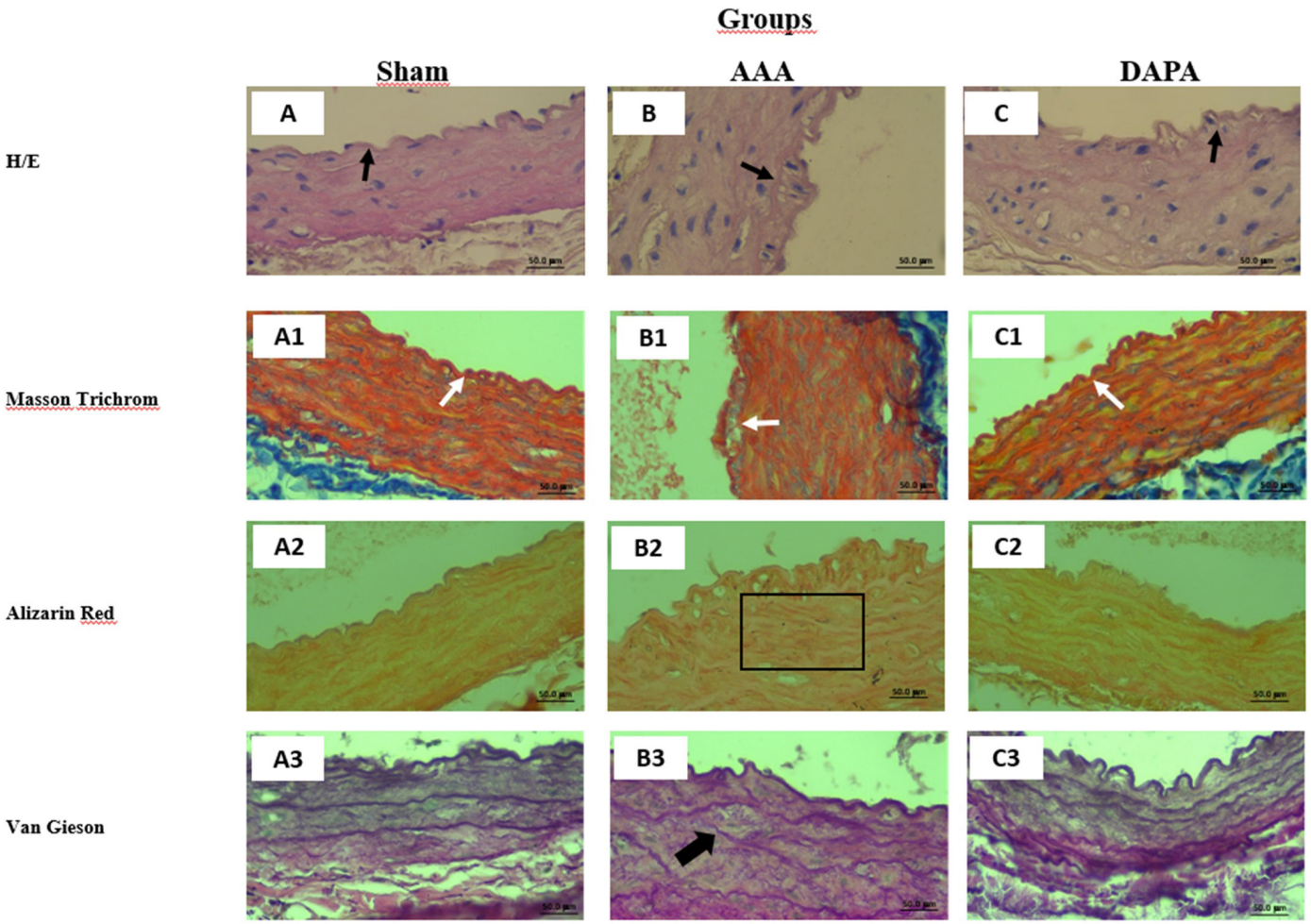

Figure 1. Group Histological sections of groups (hematoxylin + eosin stain, 40X): A - sham group, B-AAA group, and C–DAPA group. Internal elastic lamina marked with arrow. Histological sections of groups (Masson's trichrome stain, 40X): A1-sham group, B1-AAA group, C1–DAPA group. Tunica intima was marked white arrow in all images for comparison. Group Histological sections of groups (alizarin red stain, 40X): A2 - sham group, B2- AAA group, C2–DAPA group. Calcium accumulation in the groups is shown in the square. Group Histological sections of groups (van gieson stain, 40X): A3-sham group, B3-AAA group, C3–DAPA group, Deteriorations in elastic fibers in the tunica media layer were seen with the black arrow

Elastin degradation was significantly increased in the AAA group compared with sham (p=0.001) and was significantly reduced with dapagliflozin treatment compared with AAA (p=0.001), though abnormalities persisted relative to sham (p=0.040). Calcium deposition showed a similar trend, being elevated in AAA compared with sham (p=0.002) and reduced in DAPA compared with AAA (p=0.012), yet still higher than sham (p=0.022) (Table 2) (Figure 1).

Caspase-3 expression was significantly elevated in AAA compared with sham (p=0.002). Dapagliflozin significantly decreased Caspase-3 levels compared with AAA (p=0.006), but values remained higher than sham (p=0.022). Caspase-9 activity was also higher in AAA compared with sham (p=0.003). Although DAPA partially reduced Caspase-9 compared with AAA, this difference did not reach statistical significance (p=0.068), and sham–DAPA comparison remained significant (p=0.009) (Table 2).

Table 2. Histopathological parameters

Parameter	Sham (Median [IQR])	AAA (Median [IQR])	DAPA (Median [IQR])	p (Sham–AAA)	p (Sham–DAPA)	p (AAA–DAPA)
Elastin degradation	1.00 (1.00–1.00)	3.00 (3.00–3.50)	2.00 (1.00–2.00)	**0.001**	**0.040**	**0.001**
Calcium deposition	1.00 (0.25–1.00)	3.00 (2.00–3.00)	2.00 (1.00–2.00)	**0.002**	**0.022**	**0.012**
Caspase 3	1.00 (0.25–1.00)	3.00 (2.50–3.00)	2.00 (1.00–2.00)	**0.002**	**0.022**	**0.006**
Caspase 9	0.50 (0.00–1.00)	3.00 (2.00–3.00)	2.00 (1.50–2.00)	**0.003**	**0.009**	0.068

Data are presented as median (interquartile range, IQR). Exact p values are provided for all comparisons where available; for tests yielding very small probabilities (below 0.001), the values are reported as p<0.001 according to the statistical output. Values of p<0.05 were considered statistically significant. Sham: sham-operated control group, AAA: abdominal aortic aneurysm group, DAPA: dapagliflozin-treated group

AAA induction resulted in pronounced morphometric enlargement, elastin degradation, calcium deposition, and apoptosis within the aortic wall. Dapagliflozin significantly mitigated most of these pathological changes, particularly morphometric dilatation, elastin degradation, calcium deposition, and Caspase-3 activity, while its effect on Caspase-9 was less prominent.

DISCUSSION

The calcium chloride aneurysm model has been used for many years by different independent researchers, and several review studies have been published on it as an established model of AAA [4]. In our study, we utilized the calcium phosphate–based AAA model defined by Yamanouchi et al., which is a modified version of the calcium chloride–induced AAA model. This model provides more rapid and greater aneurysmal dilatation. Application of calcium phosphate to the vascular wall induces inflammation in the aortic wall. As a result, fusiform AAA develops, characterized by lumen and aortic diameter expansion accompanied by thickening of the vascular wall [5]. The $CaPO_4$ protocol leads to aortic dilatation associated with elastic fiber loss, reduction in vascular smooth muscle cells (VSMCs), inflammation, and calcium accumulation. Standardized protocols and applications of this model emphasize predictable expansion and distinct histopathological changes in a short time frame. In our findings, the increase in all area indices in the AAA group and the significant reductions with dapagliflozin demonstrated that the expected expansion trajectory in the $CaPO_4$ model was morphometrically attenuated, consistent with the reference pattern of the protocol [6].

In experimental AAA studies, disease severity and progression are generally evaluated through maximum aortic diameter, as it is the most widely used clinical measure for predicting rupture risk. However, area-based parameters such as lumen area, lumen–intima area, and lumen– intima–media area not only reflect dilatation but also structural changes in the vascular wall. This method reveals regionally heterogeneous or irregularly developing dilatations more sensitively. Furthermore, studies in small animal models have demonstrated that such area based measurements are reproducible and propose them as complementary to diameter assessments in experimental research [9]. While lumen area reflects only intraluminal geometry, the lumen–intima area quantifies potential intimal contribution. The lumen–intima– media area, targeting both total wall and lumen cross-section, integrates the degree of dilatation and the balance of medial thinning or thickening into a single parameter. In $CaPO_4$-based studies, diameter and area assessments, together with elastin-related wall integrity and calcification, enable simultaneous interpretation of morphometric and histopathological status [10].

In our study, the increase in lumen–intima–media area demonstrated the presence of aneurysmal dilatation as evaluated by external aortic diameter, while the increases in lumen and lumen+intima areas indicated that dilatation was not confined to the aortic wall but also involved luminal diameter expansion. Dapagliflozin treatment significantly reduced both the external aortic diameter and luminal expansion in these measurements. The load-bearing elastic skeleton of the aortic media determines the recoil capacity of the arterial wall. Disruption of elastin integrity, whether by fragmentation or thinning, reduces wall stability and increases the tendency for dilatation. Human aortic and aneurysm literature clearly demonstrates that alterations in elastin fiber architecture are strongly associated with aneurysmal wall weakness [11]. In experimental models, intraluminal administration or external elastase exposure directly induces fragmentation of elastic laminae and triggers aneurysmal dilatation [12]. Elastin degradation occurs not only in enzyme-mediated models such as elastase-induced

aneurysm but also in calcium phosphate models [5]. The $CaCl_2$ application underlying our model produces elastin breaks in the rat infrarenal aorta [13]. The $CaPO_4$ modification results in marked aneurysmal dilatation and medial damage within a short time, with accelerated histopathological progression and medial mineralization described at early stages. Therefore, it provides a sensitive platform for semi-quantitative monitoring of elastin integrity disruption. In our study, elastin degradation assessed by Van Gieson staining was most severe in the aneurysm group, while dapagliflozin treatment significantly reduced elastin loss. Dapagliflozin has also been reported to mitigate elastin degradation and slow aneurysm progression in a dissecting aneurysm model [14]. Although diabetes has been reported to be inversely associated with AAA presence, this may be attributable to diabetes itself or to antidiabetic medications [15,16]. The use of metformin, an antidiabetic agent distinct from SGLT-2 inhibitors, has been associated with decreased AAA prevalence [17].

Therefore, whether the anti-aneurysmal effect of dapagliflozin is independent of its antidiabetic drug class requires further investigation. In experimental models based on periadventitial calcium phosphate application, calcification is not merely an accompanying finding of aneurysm development but a fundamental component of pathological progression [18]. Mineral deposition within the vascular wall particularly accumulates on elastin and collagen fibers, reducing their elasticity and compromising the mechanical resilience of the aorta. The resultant micro-calcification foci generate heterogeneous stiff regions within the wall, leading to localized stress concentrations and fragile zones [19]. When combined with vascular smooth muscle cell apoptosis, the reparative capacity of the medial layer declines, further undermining wall structural integrity [20]. The frequent coexistence of calcification with inflammatory cell infiltration accelerates matrix degradation and enhances aneurysm progression by promoting proteolytic enzyme release [4]. Thus, calcium accumulation demonstrated in $CaCl_2$ and $CaPO_4$ models is considered a critical mechanism directly contributing to accelerated dilatation and wall destabilization. In our study, calcium deposition increased in the AAA group but was reduced with dapagliflozin. This finding indicates that calcium accumulation in our model was not merely a technical outcome of the $CaPO_4$ protocol but also a pathological hallmark consistent with the phenotype of this model, which was attenuated by dapagliflozin. In human AAA walls, calcification is highly prevalent and reported as a prominent component in most series. Moreover, increased calcification burden has been associated with overall cardiovascular risk and events.

Therefore, increased Alizarin Red (AR) positivity in experimental aneurysm models is not only a pathological correlate but also a clinically relevant histological feature [21]. In abdominal aortic aneurysm models, activation of the intrinsic apoptotic pathway is closely linked to the loss of vascular smooth muscle cells, a critical component of the medial layer. In elastase-based and other models, increases in Caspase-9, the initiator of apoptosis, and Caspase- 3, the executioner of apoptosis, are recognized as clear markers of medial cell death. Their activation reduces the reparative capacity of the medial layer and facilitates aneurysm progression. Accordingly, apoptosis has repeatedly been confirmed as an active contributor in experimental aneurysm models [22,23]. In our study, Caspase-3 and Caspase-9, representing different steps of the apoptotic process, were evaluated separately. Compared to the sham group, the AAA group exhibited increased levels of both parameters, indicating that the intrinsic apoptotic pathway actively participates in aneurysm development. However, dapagliflozin treatment did not significantly reduce Caspase-9 levels, suggesting that the drug does not exert a direct effect on the initiation phase of apoptosis. By contrast, Caspase-3 levels were significantly decreased in the treatment group compared to the AAA group, demonstrating that dapagliflozin acts predominantly at the execution phase of apoptosis. This differential effect pattern reflects the complex regulation of the apoptotic pathway and, in line with experimental and human data reported in the literature, underscores the critical role of vascular smooth muscle cell loss in AAA progression [22].

This study has certain limitations. Although the calcium phosphate model provides accelerated and reproducible aneurysm formation, it is only one of the experimental aneurysm models and addresses human AAA from a limited perspective. It does not fully reflect the slow and multifactorial development of AAA, which is influenced by long-term hemodynamic stress, systemic risk factors, and genetic predisposition. Furthermore, our evaluation was restricted to selected histopathological parameters, including morphometric indices, elastin degradation, calcium deposition, and apoptosis markers. Other relevant mechanisms, such as oxidative stress, inflammation, extracellular matrix remodeling, and biomechanical wall stress, were not assessed.

Finally, although dapagliflozin demonstrated protective effects in this preclinical model, caution is warranted in extrapolating these findings to humans due to differences in vascular biology and drug metabolism. The relatively small number of animals per group, which was determined in accordance with the principles of reduction in animal research, may limit the statistical power of the study.

CONCLUSION

In conclusion, this experimental study demonstrated that dapagliflozin attenuates aneurysmal dilatation, elastin degradation, vascular calcification, and apoptotic activity in a calcium phosphate–induced rat model of abdominal aortic aneurysm. These findings suggest that dapagliflozin exerts

protective effects on vascular integrity beyond its metabolic actions. While further research is needed to confirm these results in long-term and translational settings, our data provide preclinical evidence supporting dapagliflozin as a potential candidate for medical therapy in abdominal aortic aneurysm.

Ethics Committee Approval: It was received from the Dokuz Eylül University Animal Experiments Ethics Committee (protocol no 72/2021) (05.01.2022).

Patient Consent for Publication: Not necessary for this manuscript.

Data Sharing Statement: The data that support the findings of this study are available from the corresponding author upon reasonable request.

Author Contributions: All authors contributed equally to the article.

Conflict of Interest: The authors declared no conflicts of interest with respect to the authorship and/or publication of this article.

Funding: The authors received no financial support for the research and/or authorship of this article.

REFERENCES

1. Isselbacher EM, Preventza O, Black JH 3rd, Beck AW, Bolen MA, Braverman AC, et al. 2022 ACC/AHA guideline for the diagnosis and management of aortic disease. Circulation. 2022;146:e334-e482.
2. Song P, Rudan D, Zhu Y, Fowkes FGR, Rahimi K, Fowkes F, et al. Global and regional preva-lence of abdominal aortic aneurysm, 2000–2021. Ann Surg. 2023;278:e509-18.
3. Golledge J. Pathogenesis and management of abdominal aortic aneurysm. Eur Heart J. 2023;44:2392-408.
4. Wang YXJ, Krishna S, Golledge J. The calcium chloride-induced rodent model of abdominal aortic aneurysm. Atherosclerosis. 2013;226:29-39.
5. Yamanouchi D, Morgan S, Stair C, Seedial S, Lengfeld J, Kent KC, et al. Accelerated aneurys-mal dilation associated with apoptosis and inflammation in a newly developed calcium phosp-hate rodent abdominal aortic aneurysm model. J Vasc Surg. 2012;56:455-61.
6. Zhang S, Yang S, Gao P, Qin H, Li J, Liu Y, et al. A calcium phosphate-induced mouse abdo-minal aortic aneurysm model: protocol. J Vis Exp. 2022;189.
7. McMurray JJV, Solomon SD, Inzucchi SE, Kober L, Kosiborod MN, Martinez FA, et al. Da-pagliflozin in patients with heart failure and reduced ejection fraction. N Engl J Med. 2019;381:1995-2008.
8. Scisciola L, Cataldo V, Polese B, Balestrieri ML, Barbieri M, Rizzo MR, et al. Anti-inflammatory role of SGLT2 inhibitors: focus on cardiovascular and kidney protection. Int J Mol Sci. 2022;23:6759.
9. Ibrahim N, Bleichert S, Klopf J, Kurzreiter G, Knöbl V, Hayden H, et al. 3D ultrasound measu-rements are highly sensitive to monitor formation and progression of abdominal aortic aneurysms in mouse models. Front Cardiovasc Med. 2022;9:944180.
10. Zhang H, Liao M, Cao M, Qiu Z, Yan X, Zhou Y, et al. ATRQβ-001 vaccine prevents experi-mental abdominal aortic aneurysms. J Am Heart Assoc. 2019;8:e012341.
11. Tsamis A, Krawiec JT, Vorp DA. Elastin and collagen fibre microstructure of the human aorta in ageing and disease: a review. J R Soc Interface. 2013;10:20121004.
12. Lu G, Su G, Davis JP, Scott EA, Bauer M, Jolivalt CG, et al. A novel chronic advanced staged abdominal aortic aneurysm murine model. J Vasc Surg. 2017;66:232-41.
13. Chen HZ, Wang F, Gao P, Pei JF, Liu Y, Xu TT, et al. Age-associated sirtuin 1 reduction in vas-cular smooth muscle links vascular senescence and inflammation to abdominal aortic aneurysm. Circ Res. 2016;119:1076-88.
14. Liu H, Wei P, Fu W, Zhang J, Zhang Y, Sun Y, et al. Dapagliflozin ameliorates the formation and progression of experimental abdominal aortic aneurysms by reducing aortic inflammation in mice. Oxid Med Cell Longev. 2022;2022:8502059.
15. D'Cruz RT, Wee IJY, Syn NL, Choong AMTL. The association between diabetes and thoracic aortic aneurysms. J Vasc Surg. 2019;69:263-8.e1.
16. Morris DR, Sherliker P, Clack R, Sayers RD, Flather M, Goodall AH, et al. Opposite associations of aortic aneurysm with blood glucose and with diabetes mellitus. Circulation. 2019;140:264-6.
17. Itoga NK, Rothenberg KA, Suarez P, Ho TV, Mell MW, Xu B, et al. Metformin prescription sta-tus and abdominal aortic aneurysm disease progression in the U.S. veteran population. J Vasc Surg. 2019;69:710-6.
18. Guo M, Ji S, Wang H, Li X, Zhang Y, Chen L, et al. Myeloid cell mPGES-1 deletion attenuates calcium phosphate-induced abdominal aortic aneurysm in male mice. Inflammation. 2025;48:288-98.
19. Raaz U, Zöllner AM, Schellinger IN, Toh R, Nakagami F, Brandt M, et al. Segmental aortic stif-fening contributes to experimental abdominal aortic aneurysm development. Circulation. 2015;131:1783-95.
20. Clarke MCH, Littlewood TD, Figg N, Maguire JJ, Davenport AP, Goddard M, et al. Chronic apoptosis of vascular smooth muscle cells accelerates atherosclerosis and promotes calcification and medial degeneration. Circ Res. 2008;102:1529-38.
21. Chowdhury MM, Zieliński LP, Sun JJ, Chowdhury K, Anwar MA, Choke E, et al. Calcification of thoracic and abdominal aneurysms is associated with mortality and morbidity. Eur J Vasc Endovasc Surg. 2018;55:101-9.
22. Chakraborty A, Li Y, Zhang C, Yang X, Chen Y, Wu D, et al. Programmed cell death in aortic aneurysm and dissection: a potential therapeutic target. J Mol Cell Cardiol. 2021;163:67-76.
23. Chen Y, He Y, Wei X, Jiang DS. Targeting regulated cell death in aortic aneurysm and dissec-tion therapy. Pharmacol Res. 2022;176:106048.